




# Searching for magnetic fields in featureless white dwarfs with the DIPOL-UF polarimeter at the Nordic Optical Telescope

A. Berdyugin<sup>1,\*</sup>, J. D. Landstreet<sup>2,3,\*</sup>, S. Bagnulo<sup>2,\*</sup>, V. Piirola<sup>1</sup>, and S. V. Berdyugina<sup>4,5,6</sup>

<sup>1</sup> Department of Physics and Astronomy, FI-20014 University of Turku, Finland

<sup>2</sup> Armagh Observatory & Planetarium, College Hill, Armagh BT61 9DG, UK

<sup>3</sup> University of Western Ontario, London, Ontario N6A 3K7, Canada

<sup>4</sup> IRSOL Istituto Ricerche Solari “Aldo e Cele Daccò”, Faculty of Informatics, Università della Svizzera Italiana, Via Patocchi 57, Locarno, Switzerland

<sup>5</sup> Euler Institute, Faculty of Informatics, Università della Svizzera Italiana, Via la Santa 1, 6962 Lugano, Switzerland

<sup>6</sup> Institut für Sonnenphysik (KIS), Georges-Köhler-Allee 401A, 79110 Freiburg, Germany

Received 26 April 2024 / Accepted 19 June 2024

## ABSTRACT

About 20% of the white dwarfs possess a magnetic field that may be detected by the splitting and/or polarization of their spectral lines. As they cool, the effective temperatures of the white dwarfs become so low that no spectral lines can be seen in the visible wavelength range. If their atmospheres are not polluted by the debris of a planetary system, these cool white dwarfs have featureless optical spectra. Until quite recently, very little was known about the incidence of magnetic fields in these objects. However, when observed with polarimetric techniques, a significant number of featureless white dwarfs reveal strong magnetic fields in their optical continuum spectra. Measuring the occurrence rate and strength of magnetic fields in old white dwarfs may help us to understand how these fields are generated and evolve. We report the results of an ongoing survey of cool white dwarfs with the high-precision broad-band polarimeter DIPOL-UF, which is deployed at the Nordic Optical Telescope on La Palma, Spain. This survey has led to the firm discovery of 13 new cool magnetic white dwarfs in the solar neighborhood so far, including six new detections that we report in this paper.

**Key words.** techniques: polarimetric – stars: magnetic field – white dwarfs

## 1. Introduction

White dwarfs (WDs) are the final evolution stage of at least 90% of all stars when the useable nuclear fuel is exhausted. These objects ( $M \sim 0.6 M_{\odot}$ ,  $R \sim 0.01 R_{\odot}$ ) are common in space around the Sun; about 150 of them are found within a distance of 20 pc (Hollands et al. 2018a). The basic evolution of a WD, which initially formed by the collapse of a stellar core, is to cool slowly on a timescale of several billion years. The physics of WDs has recently been reviewed by Saumon et al. (2022). This evolution is found to be surprisingly complex, for example because magnetic fields are present in more than 20% of the WDs (e.g., Bagnulo & Landstreet 2021).

Magnetic fields have been detected in several hundred nearby WDs, mostly through Zeeman splitting of spectral lines that were observed in flux spectra (e.g., Ferrario et al. 2020). The fields cover a wide range of strengths, from below  $10^4$  G up to nearly  $10^9$  G. In a volume-limited survey within 20 pc around the Sun, fields were detected in 20–25% of the WDs that were surveyed (Bagnulo & Landstreet 2021). The fields do not appear to evolve with time on an observable timescale, but they are often not symmetric about the rotation axis of the host WD and thus appear to vary periodically as the star rotates. A geometrical model for a star with a dipolar field that is tilted with respect to

the rotation axis was developed for the magnetic Ap and Bp stars by Stibbs (1950), and is still used to describe many magnetic WDs (see, e.g., Bagnulo et al. 2024). In this respect, magnetic WDs (MWDs) are rather similar to the small fraction ( $\sim 7\%$ ) of magnetic upper main-sequence stars (magnetic Ap, Bp and O stars: see, e.g., Donati & Landstreet 2009), which also exhibit stable magnetic fields with a typical strength of about 1–100 kiloGauss (kG). These intrinsically stable fields are referred to as “fossil fields”. That these fields exist in only a fraction of WDs and of upper main-sequence stars, that is, in settings without obvious dynamo activity, is one of the outstanding physical puzzles of stellar evolution.

Studies of volume-limited samples of MWDs have revealed two specific evolution paths. (1) WDs resulting from single-star evolution, with typical masses of about  $0.6 M_{\odot}$ , only very rarely reveal detectable fields during at least the first billion years (Gyr) of cooling, and the fields observed in these young WDs are almost always very weak, typically tens or hundreds of kG. As the WDs cool, after about 2–3 Gyr, the fields begin to appear much more frequently and with much greater field strength (Bagnulo & Landstreet 2022). (2) The most massive WDs, with masses above perhaps  $1.1 M_{\odot}$ , are probably produced by WD-WD binary mergers (Tout et al. 2008; Briggs et al. 2015; García-Berro et al. 2012). These massive WDs are usually strongly magnetic from nearly (or exactly) the moment of the merger, with fields of many megaGauss (MG) and very short rotation periods (Bagnulo & Landstreet 2022).

\* Corresponding authors; andber@utu.fi, jlandstr@uwo.ca, Stefano.Bagnulo@Armagh.ac.uk

Intermediate-mass WDs probably represent a mixed population with a variety of origins, and may frequently result from binary evolution.

However, our observational understanding of the later evolution of magnetic fields in WDs that are older than a cooling age of about 5 Gyr is extremely limited. By this age, most magnetic WDs no longer display detectable Balmer lines (He lines disappear at a much younger age), which are commonly employed for detecting a magnetic field through spectral lines. If, however, WDs are metal polluted from accretion of circumstellar debris (often classified as DZ WDs), metal lines can be employed (Hollands et al. 2017, 2018b; Kawka et al. 2019). Alternatively, the magnetism of cool carbon-rich WDs with strong carbon-based molecular bands, classified as DQ WDs, can be studied using polarization in CH molecular bands when they are detectable, e.g., Angel & Landstreet (1972), Berdyugina et al. (2007), and Vornanen et al. (2013). In the remaining featureless cool WDs, which are classified as DC WDs, broad-band polarimetry may be employed. This technique has hardly been used for magnetic field searches since the 1970s (Angel et al. 1981). After these earliest works, the only discoveries of magnetic DC WDs were those made with spectropolarimetry by Putney (1997) and by Bagnulo & Landstreet (2020). Before the survey of magnetic WDs in the local 20 pc volume was completed (Bagnulo & Landstreet 2021), only 10 of the 30 DC WDs in this volume (the nearest and brightest DC WDs) had been searched for evidence of magnetism, and virtually none of the fainter, more distant DCs had been studied. This lack of data meant that we had almost no information about the presence of magnetic fields in the commonest spectral class of the oldest WDs. Hence, the magnetism in WDs that was produced during the first half of the age of the disk of the Milky Way was almost completely unknown territory.

In order to fill some of this information void, we are carrying out a systematic survey of optical circular polarization of known and suspected DC WDs in the northern hemisphere (Berdyugin et al. 2022, 2023). Here, we present a compilation of more than 110 new observations obtained for 84 WDs in 2022 July, 2023 November, and 2024 February with the high-precision three-band polarimeter Double Image Polarimeter – Ultra Fast (DIPol-UF) deployed on the Nordic Optical Telescope (NOT), located at the Observatorio del Roque de los Muchachos on the Canary Island of La Palma, Spain, including six new detections of magnetic DC WDs.

## 2. Observations

New broad-band circular polarization (BBCP) measurements were obtained from 2023 March – 2024 February using the DIPol-UF three-band polarimeter on the 2.5-m NOT. This instrument has been described in detail by Pirola et al. (2021). Briefly, we obtain measurements of broad-band circular polarization in three bands with DIPol-UF (which we call  $B'$ ,  $V'$ ,  $R'$ ), each about 1000 Å wide, centered on the wavelengths 4450 Å, 5400 Å, and 6400 Å. These bands are defined by sharp-cutoff dichroic filters with a transmission of about 90% across most of each band (see Fig. 1 of Berdyugin et al. 2022). The stability, sensitivity, and zeropoint errors of DIPol-UF have been studied extensively using observations of bright standard stars and WDs with known circular polarization properties, and it is clear that we can reliably detect polarization levels down to 0.01% with a precision and accuracy of 0.002% at least. In practice, the precision of the survey is mainly limited by the photon number from each tar-

get WD at a given telescope (Pirola et al. 2021; Berdyugin et al. 2022).

### 2.1. Observations of standard stars

During our observing run, we obtained measurements of various bright nonpolarized nearby stars to calibrate the instrumental polarization. In addition, we observed the well-known MWD WD 1900+705, which appears to show a signal of circular polarization that is nearly constant with time (see, e.g., Bagnulo & Landstreet 2019).

The measurements of unpolarized stars yield an instrumental polarization to a precision better than  $10^{-5}$  (a few parts per million). In the  $B'V'R'$  bands, the values of the reduced Stokes parameter  $V/I$  are  $0.0121 \pm 0.0004\%$ ,  $0.0109 \pm 0.0005\%$ , and  $0.0084 \pm 0.0004\%$ , respectively. This instrumental polarization was subtracted from the measured polarization of all targets.

### 2.2. Science targets

Most DC WDs have relatively low effective temperature  $T_{\text{eff}}$  values, often lower than 5000 K, and the nearest DC WDs mostly have *Gaia*  $G$  magnitudes of 15 or fainter. All our targets were chosen based on the recent nearly complete survey of spectral types and physical parameters of northern WDs within 40 pc of the Sun (McCleery et al. 2020; O'Brien et al. 2024). By expanding our survey to a volume within roughly 40 pc of the Sun, we reach typical magnitudes of 17 or even fainter for the most interesting (oldest) DCs. This is near or beyond our limiting magnitude for the desired measurement uncertainty level.

Table 1, “Basic parameters of stars observed”, available at the CDS gives the list of DC WDs that we observed during four observing runs on the NOT in 2022 November, 2023 March and November, and 2024 February. We also included some observations that were obtained in a previous run in July 2022, which were not published in our previous papers because of an oversight. The target names are listed according to the (frequently unofficial but convenient) Villanova designation (McCook & Sion 1977, 1999), followed by the main *Simbad* identifier, the *Gaia*  $G$  magnitude and distance, and various stellar parameters derived from O'Brien et al. (2024), Gentile Fusillo et al. (2021), and Bédard et al. (2020). Column 8 of Table 1, labeled “Composition” shows the spectral class of the WD when it is different than DC, using the classification by O'Brien et al. (2024) (see below). In addition to targets that were never observed before, our list includes a number of WDs in which a magnetic field has been detected in previous studies, namely WD 0004+122 (Bagnulo & Landstreet 2020); WD 0548–001 (spectral class: DQp Landstreet & Angel 1971); WD 0756+437 (Putney 1997); WD 1008+290 (spectral class: DQ, Schmidt et al. 1999); WD 1036–204 (spectral class: DQ, Liebert et al. 1978); WD 1315+222 (Berdyugin et al. 2022); WD 1346+121 (Berdyugin et al. 2023); WD 1556+044 (Berdyugin et al. 2022); WD 2049–222 (Berdyugin et al. 2022); WD 2049–253 (Bagnulo & Landstreet 2020); WD 2211+372 (Berdyugin et al. 2023). These observations served to confirm detection, to further verify the instrument reliability and stability, and to set a baseline for future studies of the rotational periods of these MWDs.

This target list includes different categories of cool WDs: He-rich and H-rich featureless WDs, and a small number of cool DQ WDs with molecular carbon ( $C_2$ ) bands. WDs with He-rich atmospheres cease to display spectral lines when the cooling has reduced  $T_{\text{eff}}$  below about 11 000 K, which occurs at a cooling

age of about 1 Gyr, and our list includes a number of DC WDs of this type that have ages of only 2–4 Gyr. In contrast, the Balmer lines of WDs with H-rich atmospheres are still visible until  $T_{\text{eff}}$  has dropped to a value of about 5000 K, which requires a cooling time of about 5 Gyr.

The resulting measurements of the broad-band circular polarization in each of the three filter bands, together with timing information, including JD, date, and time at the middle of each observation, and the total exposure time of each target, are listed in Table 2, “Observing log of WDs”, available online at the CDS. Each observation consisted of a long series of 30 s to 60 s exposures. We report in Table 2 the average of these series values, hereafter called measurements, while the mean quadratic error from the individual exposures of a given series was used to estimate the measurement error. Additional details of the data acquisition and reduction are discussed in Berdyugin et al. (2022).

Inspection of Table 2 shows that for the hotter targets, the uncertainties tend to be similar across all three bands, and they tend to be smallest in the red  $R'$  band for the cooler WDs. For obvious reasons, the uncertainties are larger for the fainter WDs, for which they sometimes rise above 0.1%. Table 2 contains observations in which two or three of the filter bands disclose polarization robustly non-zero at more than the  $3\sigma$  level, as well as isolated entries in which a single filter provides a marginally  $3\sigma$  result. We considered that we detected nonzero circular polarization either (1) when more than one measurement in any filter band exceeded a significance of  $3\sigma$ , or (2) when a single measurement was obtained with a significance of  $5\sigma$ . With these criteria, we detected fields in 6 of the 75 new WDs reported in this study. Two of the six fields we detected were further confirmed by the detection of similar polarization levels in two successive measurements. The new magnetic WDs discovered in this survey are discussed individually in the following section of this paper.

### 3. Results

#### 3.1. Newly discovered magnetic WDs

Among the stars that were observed for the first time in this survey, we detected a nonzero signal of circular polarization in six WDs: WD 0004+337 = LP 240–29; WD 0019+423 = EGGR 459; WD 0021+683 = G 242–54B; WD 0419+576 = LP 84–16; WD 0654+059 = 2MASS J06572938+0550479; and WD 0745+115 = SDSS J074842.48+112502.0. Their polarization as a function of the broad-band filters is shown in Fig. 1. We comment on the newly discovered stars below. In addition, we comment on the known very strong field MWD WD 0745+115, which shows short-term variability.

##### 3.1.1. WD 0004+337

This WD was originally identified by Luyten (1995) as a nearby object based on its high proper motion. It was classified as a probable DC WD by Limoges et al. (2015) and was confirmed using *Gaia* data by Gentile Fusillo et al. (2019, 2021). Spectral class DC and physical parameters were determined by Blouin et al. (2019). Most recently, the physical parameters have been slightly revised by O’Brien et al. (2024). Because  $T_{\text{eff}}$  is significantly above 5000 K without any trace of  $H\alpha$ , it is assumed to have a He-rich atmosphere. The cooling age of this DCH star is estimated to be nearly 5 Gyr (the letter H after the spectral type DC means that the WD is magnetic).

We only observed this WD once, but nonzero polarization at about the 0.5% level was observed in the  $B'$  filter at the 9 $\sigma$

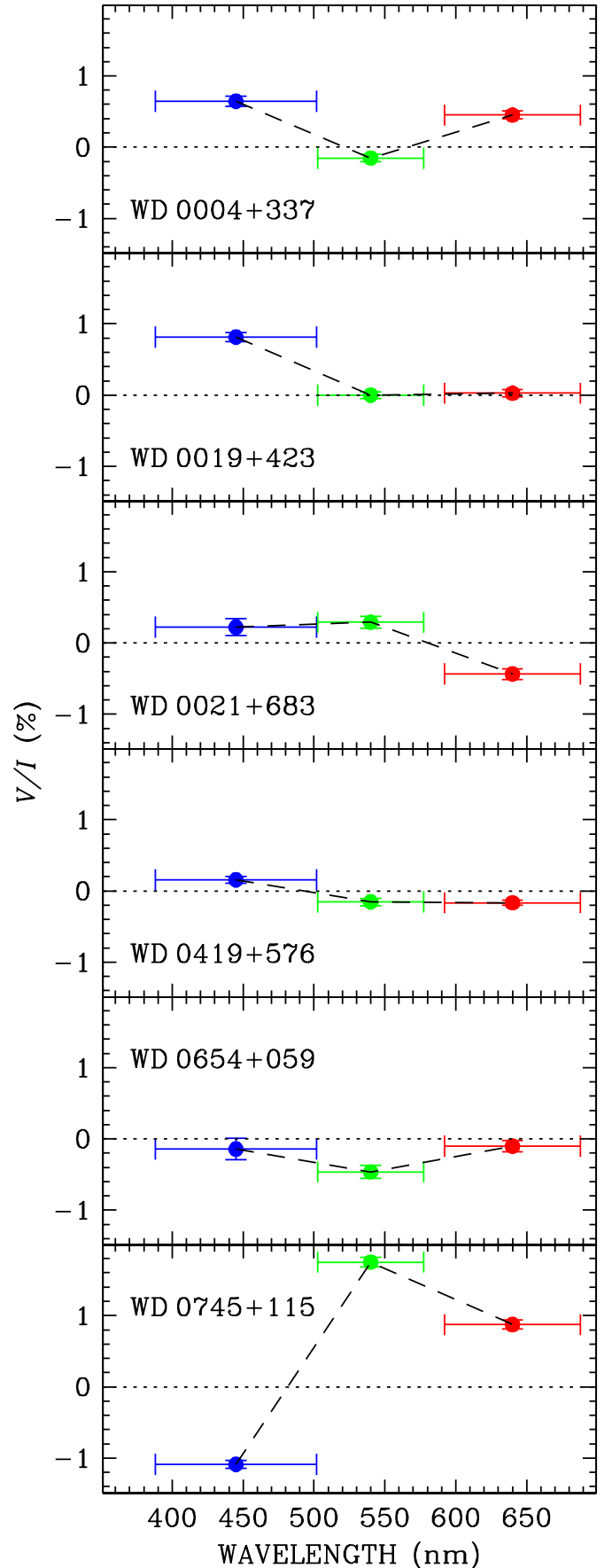


**Fig. 1.** Wavelength dependence of the circular polarization for the six newly detected magnetic WDs.



level and in the  $R'$  filter at the  $8\sigma$  level. We therefore regard this detection as quite secure. The polarization detected in both filters has the same sign. However, remarkably, a barely detectable polarization level (at  $3\sigma$ ) was observed in the  $V'$  filter.

### 3.1.2. WD 0019+423

This object, first identified as a WD by Greenstein (1979), has been included in numerous studies. Its parameters have most recently been derived by O'Brien et al. (2024), who considered it to have a DC spectrum with a He-rich atmosphere. However, with a derived mass of only  $0.39 M_{\odot}$ , which is slightly below the lowest mass that can be produced by single-star evolution, we suspect that this object may be an undetected binary pair of two similar WDs.

Circular polarization is detected at roughly the 0.8% level only in the  $B'$  band, but the observed value is nonzero at the  $12\sigma$  level, and the detection is therefore very secure. If our suspicion of binarity is correct and roughly half the light is contributed by a nonpolarized WD, the typical polarization levels in the band showing clear nonzero polarization could be near the 1.6% level. In any case, the broad-band variation of the polarization is rather similar to that of WD 0004+337 above.

### 3.1.3. WD 0021+683

This WD is the fainter member of a common-proper-motion binary with a separation of about 5 arcsec. The companion is a very cool star some three mag brighter than the WD, presumably an M dwarf. The object was identified as a WD by Gentile Fusillo et al. (2019) and was observed spectroscopically by Tremblay et al. (2020). It is included in the 40 pc WD sample (McCleery et al. 2020; O'Brien et al. 2024). It appears to have a He-rich atmosphere and an age of more than 5 Gyr.

Circular polarization is only detected with high confidence in the  $R'$  band, where the polarization of 0.435% provides a detection at nearly the  $6\sigma$  level. Polarization is also detected in the  $V'$  band at the  $3.5\sigma$  level, so that the field in this star is considered to be reliably detected, but is close to the threshold for a reliable detection with our telescope and instrument.

This WD shows only weak polarization in the  $B'$  band and appears to have a BBCP spectrum that changes sign at a wavelength between the  $R'$  band and the two bluer bands.

### 3.1.4. WD 0419+576

This object is a relatively warm DC WD with a cooling age of about 2.5 Gyr. It was identified as a WD candidate from the *Gaia* DR2 data (Jiménez-Esteban et al. 2018). A spectrum obtained by Tremblay et al. (2020) led to a clear identification as a DC WD. The WD is within the 40 pc volume (McCleery et al. 2020; O'Brien et al. 2024).

The absolute value of the observed circular polarization signal is consistently about 0.15% in the three bands, but it changes sign between the  $B'$  and the other two bands. In the  $B'$  and  $V'$  bands, the signal is only detected at about the  $3\sigma$  level, but in the  $R'$  band, the detection is at the  $5\sigma$  level, and we consider that the detection of a field is secure, if uncomfortably close to our detection limit. The magnetic field of this DCH star is probably somewhat weaker than those of the three WDs discussed above.

### 3.1.5. WD 0654+059

This object is a recently discovered nearby WD. It was first identified in the *Gaia* DR2 release by Jiménez-Esteban et al. (2018). The WD is located within the local 40 pc volume, and the physical parameters were estimated by Gentile Fusillo et al. (2019, 2021), McCleery et al. (2020), O'Brien et al. (2024). A flux spectrum was obtained by Tremblay et al. (2020), which resulted in the DC classification.

Three band polarization measurements were obtained during two winter runs. Polarization was clearly detected first in one band and then in two bands, and finally (by substantially increasing the total time on target), in all three bands. However, a close examination of the measured polarization values obtained during the three measurements does not reveal any clear temporal variation between them within the measurement errors. It appears that all three bands report polarization values of the same sign, but the  $V'$ -band polarization value is higher by about 50% than the values found in the other two bands. The highest Stokes  $V/I$  value we found is just below 0.5%.

### 3.1.6. WD 0745+115

Like several of the targets in this section, WD 0745+115 is a very recent addition to the list of relatively nearby WDs, although it lies outside the 40 pc volume. It was identified as a nearby WD by Jiménez-Esteban et al. (2018), an identification confirmed by Gentile Fusillo et al. (2019). A spectrum was obtained by Kilic et al. (2020), who identified the WD as a DC star. The basic parameters were derived by Gentile Fusillo et al. (2019, 2021), who reported that it has a relatively high mass of  $0.93 M_{\odot}$  and an effective temperature  $T_{\text{eff}}$  close to 10 000 K. For this WD, the absence of Balmer lines is a very clear indication of a He-rich atmosphere.

Strong circular polarization is present in all observed bands. The polarization approaches +2% in the  $V'$  band, is close to +1% in the  $R'$  band, and reverses sign and exceeds  $-1\%$  in the  $B'$  band. There is no significant indication of variability in the four measurements taken during about one year.

### 3.1.7. WD 0756+437

WD 0756+437 was observed as an extremely interesting target of opportunity that was easily included in our general program. The star was originally identified as a DF-C WD with a possible  $\lambda 4670 \text{ \AA}$  feature (Greenstein et al. 1977; Greenstein 1979). It was repeatedly observed photometrically and spectroscopically since then, especially after the polarimetric discovery of a large magnetic field (see below). Putney (1995) identified the object as a DA WD with a H-rich atmosphere on the basis of the comparison of features in the polarization spectrum with the theoretical spectrum of H. The star is within the 40 pc volume around the Sun (McCleery et al. 2020; O'Brien et al. 2024).

An extremely high level of circular polarization that rises to the huge value of  $V/I \sim 8\%$  at around  $5500 \text{ \AA}$  was discovered by Putney (1995), who published a single (nearly featureless) flux spectrum and an excellent circular polarization spectrum. The observed polarization level indicates that this WD possesses a very strong field. Our broad-band Stokes  $V/I$  measurements are fully consistent with Putney's data.

Putney compared narrow polarization features with predicted wavelength positions of various components of  $H\alpha$  in fields of hundreds of MG (Wunner et al. 1985) and concluded that the mean ( $\langle |B| \rangle$ ) field must be about 200–220 MG in strength.

This field strength was also supported by Schmidt et al. (2003) on the basis of SDSS intensity spectra. Comparison of the spectral energy distribution with models (Limoges et al. 2015; Gentile Fusillo et al. 2021) suggests that  $T_{\text{eff}} = 7215 \text{ K}$ ,  $M = 1.04 M_{\odot}$ , and that the cooling age is about 4.45 Gyr. This DAH WD is thus probably (one of?) the oldest known, strongly magnetized products of a WD-WD merger (García-Berro et al. 2012; Bagnulo & Landstreet 2022).

We took five polarization data sets during two years. From the fact that the first two measurements, taken about 3 h apart, also provide the highest and lowest polarization values in our measurement set, we deduce that the rotation period of this star could be on the order of six hours. Photometry by Brinkworth et al. (2013) showed very large amplitude sinusoidal photometric variations (semi-amplitude of  $\pm 4\%$ ) with a unique period of 6.68 h. Because the polarimetric variations are due to and locked to the stellar rotation, the agreement of the polarimetric period constraints with the photometric period confirms that the photometric period is the stellar rotation period.

### 3.2. Other targets with marginal detections

In addition to these reasonably certain detections, the observations of nine other DC WDs provided a single detection at or slightly above the  $3\sigma$  level in one band. These WDs can be regarded as candidates that need further measurements for a confirmation. They are WD 0052+595; WD 0102+210; WD 0156+155; WD 0357+513; WD 0407+197; WD 0426+588; WD 1554-079; WD 1731+290. Because of previous experience with unsuccessfully trying to confirm magnetic fields based on a single  $3\sigma$  polarization detection (see Sect. 3.3 below), we suspect that the majority of these detections will not be confirmed, except perhaps for the case of WD 0052+595.

### 3.3. Targets with unconfirmed detections

In our previous observing runs, polarization was detected once in a single band at a level slightly higher than  $3\sigma$  in observations of WD 1434+437 and WD 1533+469 (Berdyugin et al. 2023). We obtained one more observation of each of these two stars that failed to confirm the marginal detections reported earlier. We dropped these stars from our list of DCH candidates.

## 4. Discussion and conclusions

The circular polarization levels detected with the DIPoL-UF at NOT range from about 1%, found in two DC WDs to a number of detections of polarization at levels between 0.2% and 0.6%, with measurement uncertainties ranging between about 0.02% to 0.1%. It is clear that an extremely important feature of the DIPoL-UF polarimeter is its stable and precisely measured zero-point (Berdyugin et al. 2022). However, our observing program reaches the limit of what can be achieved with a medium-sized telescope such as the 2.5 m NOT. Further substantial progress will require the use of larger telescopes.

Figure 2 shows the relation of the magnitude and the uncertainty of our measurement errors of all NOT+DIPoL-UF measurements of WDs as a function of *Gaia*  $G$  magnitude, normalized to 1 h exposure time. This figure represents a substantial update compared to Fig. 4 of Berdyugin et al. (2022). It may be used to make quantitative predictions regarding the level of polarimetric precision that may be achieved for the BBCP measurements as a function of exposure time and stellar magnitude.

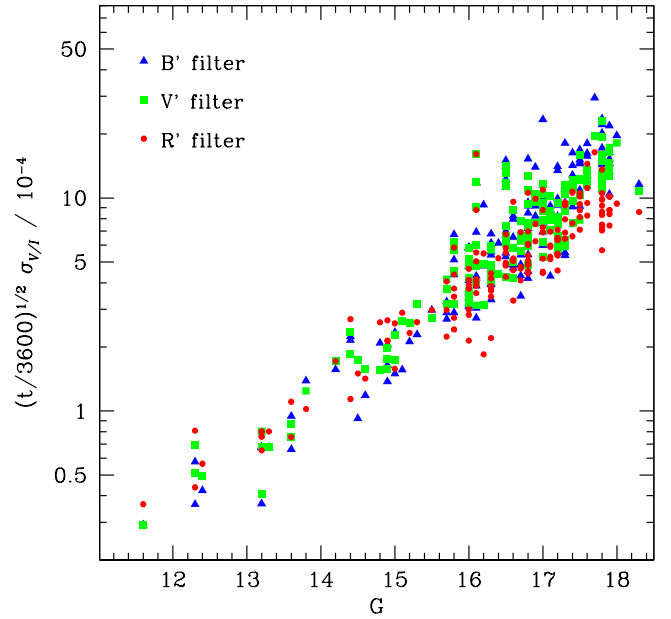


**Fig. 2.** Relation of the magnitude and measurement errors of all DIPoL-UF measurements of WDs at NOT as a function of *Gaia*  $G$  magnitude, normalized to 1 h exposure time.

It can also be used to evaluate observational requirements for a given WD with DIPoL-UF employed on a larger telescope.

Our search for broad-band circular polarization, and therefore, for magnetic fields, in DC WDs continues to deliver detections of previously unknown fields in these faint and featureless objects, with a detection rate of 13 new MWDs so far out of 101 observed new targets. The diverse outcome obtained in our different runs is remarkable: Berdyugin et al. (2022) reported the detection of 2 new MWDs out of 3 newly observed DC WDs, Berdyugin et al. (2023) reported 5 out of 23, and we detected and reported 6 new MWDs out of 75. Overall, the detection of a magnetic field in 13 out of 105 observed WDs is fully consistent with the frequency of the occurrence of magnetic fields in the DC WDs in the local 20 pc volume,  $13.3 \pm 6.2\%$ , that was measured by Bagnulo & Landstreet (2021). This value is certainly an underestimate of the actual frequency of magnetic fields in old WDs because stars with magnetic fields weaker than a few MG do not produce a signal of circular polarization that can be detected with our instruments. On the other hand, only 2 of the newly discovered magnetic DC stars show circular polarization levels in excess of 1%. We found no new magnetic DC WDs with extremely high polarization levels in our survey (several percent polarization), similar to those found in other types of magnetic WDs, such as WD 1900+705 (=Grw+70° 8247,  $\sim 3\%$ , Kemp et al. 1970), WD 0756+437 (=EGGR 428,  $\sim 8\%$ , Putney 1995), CL Oct (=EUVE J0317-85.5,  $\sim 11\%$ , Barstow et al. 1995), and WD 1031+234 (=PG 1031+234,  $\sim 12\%$ , West & Schmidt 1984; Latter et al. 1986; Schmidt et al. 1986). Our new data, combined with spectropolarimetric surveys of WDs of various cooling ages, will eventually help us to understand the origin and evolution of magnetic fields in degenerate stars.

We note that roughly half of the DCs observed in this survey belong to the category of younger DCs that have He atmospheres,  $T_{\text{eff}} \gtrsim 6000 \text{ K}$ , and cooling ages younger than about 4 Gyr. These stars were presumably DB WDs earlier in their cooling. The other, older, DCs, also about half of the sample,

with lower  $T_{\text{eff}}$  values and ages older than about 4 or 5 Gyr, may have H-rich or He-rich atmospheres, and these stars sample the production of magnetic WDs during the first few billion years of the evolution of the Milky Way galaxy.

We cannot assign definite magnetic field strengths to the observed polarization signals because the theory of continuum circular polarization in these very cool WDs has not been studied in detail. However, using a rough estimate (derived from somewhat hotter magnetic WDs) that polarization  $V/I \sim 1\%$  is produced by a mean line-of-sight field component  $\langle B_z \rangle$  of about 15 MG (Bagnulo & Landstreet 2020), most of the fields detected in our survey probably have overall typical field strengths  $\langle |B| \rangle$  of a few MG to tens of MG, rising to perhaps as high as 100 MG in the most highly polarized WDs.

The magnetic fields of DC WDs have been an almost completely neglected topic since the 1970s, when searches with broad-band polarimetry went out of fashion. We showed that this method of searching for fields in these generally faint WDs is still an extremely powerful tool that has revealed MG-level fields in a significant fraction of the DCs. These newly discovered magnetic DC WDs can now be studied with spectropolarimetry using larger telescopes, which will provide additional constraints for developing a suitable model for their enigmatic circularly polarized continuum spectra.

## Data availability

Tables 1 and 2 are available at the CDS via anonymous ftp to [cdsarc.cds.unistra.fr](https://cdsarc.cds.unistra.fr) (130.79.128.5) or via <https://cdsarc.cds.unistra.fr/viz-bin/cat/J/A+A/690/A10>

*Acknowledgements.* Based on observations made with the Nordic Optical Telescope, owned in collaboration by the University of Turku and Aarhus University, and operated jointly by Aarhus University, the University of Turku and the University of Oslo, representing Denmark, Finland and Norway, the University of Iceland and Stockholm University at the Observatorio del Roque de los Muchachos, La Palma, Spain, of the Instituto de Astrofísica de Canarias. DIPol-UF is a joint effort between University of Turku (Finland) and Leibniz Institute for Solar Physics (Germany). We acknowledge support from the Magnus Ehrnrooth foundation and the ERC Advanced Grant HotMol ERC-2011-AdG-291659. JDL acknowledges the financial support of the Natural Sciences and Engineering Research Council of Canada (NSERC), funding reference number 6377-2016.

## References

Angel, J. R. P., & Landstreet, J. D. 1972, *ApJ*, 178, L21  
 Angel, J. R. P., Borra, E. F., & Landstreet, J. D. 1981, *ApJS*, 45, 457  
 Bagnulo, S., & Landstreet, J. D. 2019, *MNRAS*, 486, 4655  
 Bagnulo, S., & Landstreet, J. D. 2020, *A&A*, 643, A134  
 Bagnulo, S., & Landstreet, J. D. 2021, *MNRAS*, 507, 5902  
 Bagnulo, S., & Landstreet, J. D. 2022, *ApJ*, 935, L12  
 Bagnulo, S., Farihi, J., Landstreet, J. D., & Folsom, C. P. 2024, *ApJ*, 963, L22  
 Barstow, M. A., Jordan, S., O'Donoghue, D., et al. 1995, *MNRAS*, 277, 971

Bédard, A., Bergeron, P., Brassard, P., & Fontaine, G. 2020, *ApJ*, 901, 93  
 Berdyugin, A. V., Piirola, V., Bagnulo, S., Landstreet, J. D., & Berdyugina, S. V. 2022, *A&A*, 657, A105  
 Berdyugin, A. V., Piirola, V., Bagnulo, S., Landstreet, J. D., & Berdyugina, S. V. 2023, *A&A*, 670, A2  
 Berdyugina, S. V., Berdyugin, A. V., & Piirola, V. 2007, *Phys. Rev. Lett.*, 99, 091101  
 Blouin, S., Dufour, P., Thibeault, C., & Allard, N. F. 2019, *ApJ*, 878, 63  
 Briggs, G. P., Ferrario, L., Tout, C. A., Wickramasinghe, D. T., & Hurley, J. R. 2015, *MNRAS*, 447, 1713  
 Brinkworth, C. S., Burleigh, M. R., Lawrie, K., Marsh, T. R., & Knigge, C. 2013, *ApJ*, 773, 47  
 Donati, J.-F., & Landstreet, J. D. 2009, *ARA&A*, 47, 333  
 Ferrario, L., Wickramasinghe, D., & Kawka, A. 2020, *Adv. Space Res.*, 66, 1025  
 García-Berro, E., Lorén-Aguilar, P., Aznar-Siguán, G., et al. 2012, *ApJ*, 749, 25  
 Gentile Fusillo, N. P., Tremblay, P.-E., Gänsicke, B. T., et al. 2019, *MNRAS*, 482, 4570  
 Gentile Fusillo, N. P., Tremblay, P. E., Cukanovaite, E., et al. 2021, *MNRAS*, 508, 3877  
 Greenstein, J. L. 1979, *ApJ*, 227, 244  
 Greenstein, J. L., Oke, J. B., Richstone, D., van Altena, W. F., & Steppe, H. 1977, *ApJ*, 218, L21  
 Hollands, M. A., Koester, D., Alekseev, V., Herbert, E. L., & Gänsicke, B. T. 2017, *MNRAS*, 467, 4970  
 Hollands, M. A., Tremblay, P.-E., Gänsicke, B. T., Gentile-Fusillo, N. P., & Toonen, S. 2018a, *MNRAS*, 480, 3942  
 Hollands, M. A., Gänsicke, B. T., & Koester, D. 2018b, *MNRAS*, 477, 93  
 Jiménez-Esteban, F. M., Torres, S., Rebassa-Mansergas, A., et al. 2018, *MNRAS*, 480, 4505  
 Kawka, A., Vennes, S., Ferrario, L., & Paunzen, E. 2019, *MNRAS*, 482, 5201  
 Kemp, J. C., Swedlund, J. B., Landstreet, J. D., & Angel, J. R. P. 1970, *ApJ*, 161, L77  
 Kilic, M., Bergeron, P., Kosakowski, A., et al. 2020, *ApJ*, 898, 84  
 Landstreet, J. D., & Angel, J. R. P. 1971, *ApJ*, 165, L67  
 Latter, W. B., Schmidt, G. D., & Green, R. F. 1986, *BAAS*, 18, 975  
 Liebert, J., Angel, J. R. P., Stockman, H. S., & Beaver, E. A. 1978, *ApJ*, 225, 181  
 Limoges, M. M., Bergeron, P., & Lépine, S. 2015, *ApJS*, 219, 19  
 Luyten, W. J. 1995, *VizieR Online Data Catalog: I/98A*  
 McCleery, J., Tremblay, P.-E., Gentile Fusillo, N. P., et al. 2020, *MNRAS*, 499, 1890  
 McCook, G. P., & Sion, E. M. 1977, *Villanova University Observatory Contributions* (Villanova: Villanova Press)  
 McCook, G. P., & Sion, E. M. 1999, *ApJS*, 121, 1  
 O'Brien, M. W., Tremblay, P. E., Klein, B. L., et al. 2024, *MNRAS*, 527, 8687  
 Piirola, V., Kosenkov, I. A., Berdyugin, A. V., Berdyugina, S. V., & Poutanen, J. 2021, *AJ*, 161, 20  
 Putney, A. 1995, *ApJ*, 451, L67  
 Putney, A. 1997, *ApJS*, 112, 527  
 Saumon, D., Blouin, S., & Tremblay, P.-E. 2022, *Phys. Rep.*, 988, 1  
 Schmidt, G. D., West, S. C., Liebert, J., Green, R. F., & Stockman, H. S. 1986, *ApJ*, 309, 218  
 Schmidt, G. D., Liebert, J., Harris, H. C., Dahn, C. C., & Leggett, S. K. 1999, *ApJ*, 512, 916  
 Schmidt, G. D., Harris, H. C., Liebert, J., et al. 2003, *ApJ*, 595, 1101  
 Stibbs, D. W. N. 1950, *MNRAS*, 110, 395  
 Tout, C. A., Wickramasinghe, D. T., Liebert, J., Ferrario, L., & Pringle, J. E. 2008, *MNRAS*, 387, 897  
 Tremblay, P. E., Hollands, M. A., Gentile Fusillo, N. P., et al. 2020, *MNRAS*, 497, 130  
 Vornanen, T., Berdyugina, S. V., & Berdyugin, A. 2013, *A&A*, 557, A38  
 West, S. C., & Schmidt, G. D. 1984, *BAAS*, 16, 945  
 Wunner, G., Roesner, W., Herold, H., & Ruder, H. 1985, *A&A*, 149, 102